Published in final edited form as:
Toxicol Appl Pharmacol. 2008 September 15; 231(3): 384–392. doi:10.1016/j.taap.2008.05.014.

Increased oxidative stress and antioxidant expression in mouse keratinocytes following exposure to paraquat

Adrienne T. Black[1], **Joshua P. Gray**[1], **Michael P. Shakarjian**[2], **Debra L. Laskin**[1*], **Diane E. Heck**[1], and **Jeffrey D. Laskin**[3]

1*Department of Pharmacology and Toxicology, Rutgers University, Piscataway, NJ 08854*

2*Department of Medicine, University of Medicine and Dentistry of New Jersey-Robert Wood Johnson Medical School, Piscataway, NJ 08854*

3*Department of Environmental and Occupational Medicine, University of Medicine and Dentistry of New Jersey-Robert Wood Johnson Medical School, Piscataway, NJ 08854*

Abstract

Paraquat (1,1'-dimethyl-4,4'-bipyridinium) is a widely used herbicide known to induce skin toxicity. This is thought to be due to oxidative stress resulting from the generation of cytotoxic reactive oxygen intermediates (ROI) during paraquat redox cycling. The skin contains a diverse array of antioxidant enzymes which protect against oxidative stress including superoxide dismutase (SOD), catalase, glutathione peroxidase-1 (GPx-1), heme oxygenase-1 (HO-1), metallothionein-2 (MT-2), and glutathione-*S*-transferases (GST). In the present studies we compared paraquat redox cycling in primary cultures of undifferentiated and differentiated mouse keratinocytes and determined if this was associated with oxidative stress and altered expression of antioxidant enzymes. We found that paraquat readily undergoes redox cycling in both undifferentiated and differentiated keratinocytes, generating superoxide anion and hydrogen peroxide as well as increased protein oxidation which was greater in differentiated cells. Paraquat treatment also resulted in increased expression of HO-1, Cu,Zn-SOD, catalase, GSTP1, GSTA3 and GSTA4. However, no major differences in expression of these enzymes were evident between undifferentiated and differentiated cells. In contrast, expression of GSTA1-2 was significantly greater in differentiated relative to undifferentiated cells after paraquat treatment. No changes in expression of MT-2, Mn-SOD, GPx-1, GSTM1 or the microsomal GST's, mGST1, mGST2 and mGST3, were observed in response to paraquat. These data demonstrate that paraquat induces oxidative stress in keratinocytes leading to increased expression of antioxidant genes. These intracellular proteins may be important in protecting the skin from paraquatmediated cytotoxicity.

Keywords

paraquat; glutathione-S-transferase; MAPEG; skin; oxidative stress

*To whom correspondence should be addressed, Debra L. Laskin, Ph.D., Department of Pharmacology and Toxicology, Ernest Mario School of Pharmacy, Rutgers University, 160 Frelinghuysen Road, Piscataway, NJ 08854, Email: laskin@eohsi.rutgers.edu.

Introduction

Occupational exposures to the herbicide paraquat (1,1'-dimethyl-4,4'-bipyridinium) has been associated with a variety of skin diseases including contact dermatitis, premalignant lesions and squamous cell carcinomas (Wang *et al.*, 1987; Vilaplana *et al.*, 1993; Jee *et al.*, 1995; Anderson and Scerri, 2003). Paraquat readily penetrates the skin, and toxicity is thought to result from the generation of reactive oxygen intermediates (ROI) through redox cycling (Bus *et al.*, 1974; Bus *et al.*, 1976; Bus and Gibson, 1984; Krall *et al.*, 1988). Previous studies have shown that paraquat redox cycling is a primary mechanism of oxidative injury in many cell types including brain, liver, kidney and lung (Tomita, 1991; Bonneh-Barkay *et al.*, 2005). During redox cycling, paraquat undergoes a single electron reduction to form a paraquat radical via NAD(P)H oxidase activity (see Fig. 1A for summary) (Bus and Gibson, 1982). The paraquat radical is rapidly oxidized back to the parent compound with the concomitant transfer of the extra electron to molecular oxygen, forming superoxide anion (Bus and Gibson, 1982). Subsequent reduction of superoxide anion generates hydrogen peroxide and, potentially, highly toxic hydroxyl radicals (Darr and Fridovich, 1994). Production of these ROI leads to intracellular oxidative stress and damage to cellular macromolecules including DNA, lipids and protein (Trouba *et al.*, 2002). Functional groups on proteins are particularly susceptible to oxidation resulting in the formation of carbonyls which can lead to adduct generation with associated altered or loss of protein function (Dean *et al.*, 1997a; Levine, 2002).

Cellular antioxidants play a key role in the removal or detoxification of ROI, which is essential for preventing oxidative damage (Yu, 1994). The epidermis of the skin contains a complex enzymatic antioxidant defense system (Darr and Fridovich, 1994) (see Fig. 1B for ROI generating and detoxification pathways). This system includes enzymes that act directly to detoxify ROI such as superoxide dismutase (SOD), catalase and glutathione peroxidase (GPx), as well as ROI scavengers such as heme oxygenase-1 (HO-1), metallothionein-2 (MT-2) (Maines and Panahian, 2001;Coyle *et al.*, 2002) and glutathione metabolizing enzymes such as the glutathione *S*-transferases (GST) (Hayes and McLellan, 1999). The skin's response to oxidative stress is multi-faceted which is due in part to the fact that it is comprised of proliferating basal keratinocytes with overlying layers of cells in various stages of terminal differentiation. Increased levels of protein oxidation and lipid peroxidation following exposure to oxidants such as ozone or ultraviolet radiation have been detected in the outermost layers of the epidermis of both mouse (Thiele *et al.*, 1997) and human skin (Theile *et al.*, 1999). The differentiation process may, therefore play a role in both the level of oxidative damage and the antioxidant response of epidermal keratinocytes.

In the present studies, we compared paraquat redox cycling in primary cultures of undifferentiated and differentiated mouse keratinocytes. We also determined if paraquat-induced oxidative stress in these cells was associated with alterations in antioxidant expression. We found that paraquat is readily metabolized by both cell types, generating ROI, and that this results in cellular protein oxidation. In both undifferentiated and differentiated keratinocytes, paraquat-induced oxidative stress resulted in upregulation of HO-1, SOD, catalase and several GST enzymes. Differentiated cells were more responsive to paraquat than undifferentiated cells. Increased oxidative stress in differentiating epidermal keratinocytes may be an important mechanism of paraquat-induced skin toxicity.

Materials and Methods

Chemicals and reagents

M-MLV Reverse Transcriptase was from Promega (Madison, WI) and collagen IV was purchased from BD Biosciences (San Diego, CA). The Western Lightning enhanced chemiluminescence kit was from Perkin Elmer Life Sciences, Inc. (Boston, MA) and precast

polyacrylamide gels were from Pierce Biotechnology, Inc. (Rockford, IL). Anti- HO-1 antibodies were purchased from Assay Designs (Ann Arbor, MI), anti-catalase antibodies were from Abcam (Cambridge, MA) and Cu,Zn-SOD antibodies from Santa Cruz Biotechnology (Santa Cruz, CA). Antibodies to keratin-1, keratin-10 and filaggrin were obtained from Covance Research Products (Berkley, CA). Horseradish peroxidase-conjugated goat anti-rabbit, detergent-compatible protein assay reagents and the Silver Stain Plus kit were from Bio-Rad Laboratories (Hercules, CA). SYBR Green Master Mix and other PCR reagents were purchased from Applied Biosystems (Foster City, CA). All cell culture media, 10-acetyl-3, 7-dihydroxyphenoxazine (Amplex Red) and 3H-phenoxazine (resorufin) were from Invitrogen Corp (Carlsbad, CA). Paraquat, protease inhibitor cocktail, NADPH and all other chemicals were from Sigma (St. Louis, MO).

Cells

Primary keratinocytes were isolated and cultured from C57Bl/6J neonatal mice as previously described (Hager *et al.*, 1999). To initiate an experiment, cells were grown on collagen IV-coated plates and cultured in serum-free low calcium (0.05 mM) Keratinocyte Growth Medium to maintain their undifferentiated phenotype. Differentiation was induced by the addition of calcium (0.15 mM) to the culture medium (Yuspa *et al*., 1988). Differentiation was confirmed by morphological changes and expression of differentiation markers including keratin 1, keratin 10 and filaggrin, as determined by Western blotting (Yuspa *et al.*, 1989). In some experiments, primary C57Bl/6J keratinocytes were purchased from the Yale University Cell Culture Facility (New Haven, CT).

Assays for ROI production

Superoxide anion was quantified by the formation of 2-hydroxyethidium from dihydroethidine as described by Zhao et al. (Zhao *et al.*, 2005). Briefly, a reaction mix containing cell lysates (150 μg/μl protein), paraquat (100 μM), NADPH (0.5 mM) and dihydroethidine (40 μM) was incubated for one h at 37°C. The reaction was stopped by the addition of an equal volume of ice-cold methanol. The samples were then centrifuged at 12,000 × *g* for 10 min at 4°C and the supernatants collected. 2-hydroxyethidium was quantified using a Shimadzu HPLC (Kyoto, Japan) fitted with a Luna C18 column (250 mm × 2.0 mm) (Phenomenex, Torrance, CA) and a Shimadzu RF-535 fluorescence detector with excitation and emission set at 510 and 595 nm, respectively. The mobile phase consisted of acetonitrile in 0.1% trifluoroacetic acid and was run by a linear increase of acetonitrile from 10% to 40% in 35 min at a flow rate of 0.2 ml/min.

The formation of hydrogen peroxide was quantified using the Amplex Red fluorescence assay as previously described (Vetrano *et al.*, 2005). Briefly, reactions were run in 96-well microtiter plates at 37° C and contained 10 μM Amplex Red reagent, 50 μM NADPH and 130–150 μg/μl of cell protein lysate in a total volume of 50 μl. The detection of the fluorescent product, resorufin, was recorded every 2.5 min for 30 min using an HTS 7000 Plus BioAssay Reader (Perkin Elmer Life Sciences, Boston, MA). In some experiments, the inhibitors dicoumarol (100 μM) or diphenyleneiodonium (DPI) (10 μM) were added directly to the reaction mix.

Assays for NADPH metabolism and formation of paraquat radical

The generation of paraquat radicals and depletion of NADPH in reaction mixtures were quantified in 0.5-ml cuvettes using a Lambda 20 UV/visible spectrophotometer (PerkinElmer Life Sciences). Paraquat radicals were quantified by increases in absorbance at 604 nm (Tampo *et al*., 1999) and were recorded on the spectrophotometer by scanning at 1 nm/s, recording at 1-nm intervals, and repeating the scan at 2.5-min intervals for 60 min. Since paraquat radicals are unstable in the presence of oxygen (Bus and Gibson, 1982), experiments were run in filled cuvettes covered tightly with Parafilm to create anaerobic conditions. The formation of the radical was confirmed by the appearance of the blue-violet paraquat radical (Michaelis and

Hill, 1933). NADPH metabolism was assayed by monitoring decreases in absorbance at 340 nm and were recorded every 2.5 min for 3 h.

Western blotting

Cell lysates were prepared using an SDS-lysis buffer (10 mM Tris-base and 1% SDS, pH 7.6 supplemented with a protease inhibitor cocktail consisting of 4-(2-aminoethyl)benzenesulfonyl fluoride, aprotinin, bestatin hydrochloride, N-(trans-epoxysuccinyl)-L-leucine 4-guanidinobutylamide, EDTA and leupeptin). Lysates containing 20 μg protein were separated on 10% SDS-polyacrylamide gels and then transferred to nitrocellulose membranes. After incubating the membranes in blocking buffer (5% dry milk Tris-buffered saline with 0.1% Tween 20) for 1 h at room temperature or overnight at 4°C, the membranes were incubated for 2 h at room temperature or overnight at 4°C with primary antibodies followed by horseradish peroxidase-conjugated secondary antibodies for 1 h at room temperature. Protein immunoreactive bands were visualized using enhanced chemiluminescence (ECL) reagents. Loading of equal amounts of protein was confirmed by silver staining of the gels.

Protein oxidation assay

Protein oxidation was determined by quantifying the formation of carbonyl groups on protein side chains (Stadtman, 1993; Chevion *et al.*, 2000; Levine, 2002; Dalle-Donne *et al.*, 2006) using an OxyBlot Protein Oxidation Detection Kit (Chemicon International, Temecula, CA). Briefly, cell lysates were treated with 2,4-dinitrophenylhydrazine to derivatize the carbonyl groups on proteins to 2,4-dinitrophenylhydrazone-tagged products. Nonderivatized samples were used as a control. Samples were separated on pre-cast 4–20% gradient SDS-polyacrylamide gels and then transferred to nitrocellulose membranes. The membranes were blocked with 1% BSA in PBS with 0.1% Tween 20 and incubated with primary antibodies to dinitrophenylhydrazone-modified carbonyl groups, followed by HRP-conjugated secondary antibodies. Protein expression was visualized using ECL reagents and loading of equal amounts of protein was confirmed by silver staining of the gels.

Real-time polymerase chain reaction (PCR)

RNA was isolated using Tri Reagent (Sigma, St. Louis, MO) following the protocol provided by the manufacturer. The RNA was converted to cDNA using M-MLV reverse transcriptase. The cDNA was diluted 1:10 in RNase-DNase-free water for PCR analysis. For each gene to be tested, a standard curve composed of a serial dilution of a pool of the cDNA from the samples was used as a reference. All values were normalized to β-actin (n = 3, ± SE). The undifferentiated control was given a value of one and the values for both the undifferentiated and differentiated samples were calculated relative to this control sample. Real-time PCR was performed on an ABI Prism 7900 Sequence Detection System using 96-well optical reaction plates. SYBR-Green was used for detection of fluorescent signal and the standard curve method was used for relative quantification analysis. The primer sequences for the genes were generated using Primer Express software (Applied Biosystems) and the oligonucleotides were synthesized by Integrated DNA Technologies, Inc. (Coralville, IA). The forward and reverse primer sequences (5'→3') were: β-actin, TCACCCACACTGTGCCCATCTACGA and GGATGCCACAGGATTCCATACCCA; catalase, ACCAGGGCATCAAAAACTTG and GCCCTGAAGCTTTTTGTCAG; GSTA1-2, CAGAGTCCGGAAGATTTGGA and CAAGGCAGTCTTGGCTTCTC; GSTA3, GCAAGCCTTGCCAAGATCAA and GGCAGGGAAGTAACGGTTCC; GSTA4, CCCTTGGTTGAAATCGATGG and GAGGATGGCCCTGGTCTGT; GSTM1, CCTACATGAAGAGTAGCCGCTACAT and TAGTGAGTGCCCGTGTAGCAA; GSTP1, CCTTGGCCGCTCTTTGG and GGCCTTCACGTAGTCATTCTTACC; GPx-1, GGTTCGAGCCCAATTTTACA and TCGATGTCGATGGTACGAAA; HO-1, CCTCACTGGCAGGAAATCATC and

CCTCGTGGAGACGCTTTACATA; MT-2, TGCAGGAAGTACATTTGCATTGTT and TTTTCTTGCAGGAAGTACATTTGC; mGST1, GCTTTGGCAAGGGAGAGAATG and CCTTCTCGTCAGTGCGAACA; mGST2, TGCAGCCTGTCTGGGTCTC and CAGAAATACTTGTGACGGGCG; mGST3, GGAGGTGTACCCTCCCTTCC and TGGTAAACACCTCCCACCGT; Cu,Zn-SOD, ACCAGTGCAGGACCTCATTTTAA and TCTCCAACATGCCTCTCTTCATC; and Mn-SOD, CACATTAACGCGCAGATCATG and CCAGAGCCTCGTGGTACTTCTC.

Statistical analysis

Data are expressed as mean ± SEM. Statistical differences between the means were determined using two-way analysis of variance (ANOVA) and were considered statistically significant at $p < 0.05$.

Results

Paraquat-induced redox cycling in keratinocytes

In initial experiments, we compared paraquat redox cycling in undifferentiated and differentiated keratinocytes by quantifying the generation of superoxide anion and hydrogen peroxide. Paraquat was found to stimulate the formation of superoxide anion in keratinocyte cell lysates as detected by the generation of 2-hydroxyethidium from dihydroethidine (Fig. 2). This was inhibited by superoxide dismutase (350 U/ml) demonstrating that the ROI was in fact superoxide anion. No major differences were observed between undifferentiated and differentiated keratinocytes. We also found that paraquat stimulated hydrogen peroxide production by keratinocytes in a time- and concentration-dependent manner (Fig. 3, upper panels). Greater activity was noted in differentiated cells, when compared to undifferentiated cells (Fig. 3, lower panels). The accumulation of hydrogen peroxide was blocked by catalase (10 U/ml), but not superoxide dismutase (400 U/ml) (data not shown), confirming the specificity of the assay. Paraquat redox cycling and ROI formation is dependent on oxidation of NAD(P)H to NAD(P)+ (Bus *et al*., 1974). We found that NADPH was rapidly metabolized to NADP+ in our enzyme assays; however, no major differences were noted between undifferentiated and differentiated cells (Fig. 4). Diphenyleneiodonium (DPI) has been shown to effectively suppress the activity of many FAD reducing enzymes (Riganti *et al.*, 2004) including NADPH oxidoreductase (O'Donnell *et al*., 1993). DPI (10 μM) was found to inhibit paraquat-induced hydrogen peroxide production in both undifferentiated and differentiated keratinocytes (Fig 5), indicating that paraquat redox cycling is catalyzed by FAD-dependent NADPH oxidoreductases. Previous studies have shown that NAD(P)H quinone oxidoreductase 1 (NQO1), an FAD-containing oxidase, can participate in redox cycling reactions (Kishi *et al.*, 2002). Dicoumarol, an inhibitor of NQO1 (Asher *et al.*, 2006), was found to suppress paraquat redox cycling in both undifferentiated and differentiated cells (Fig. 5).

During redox cycling paraquat is reduced to a radical (Fig. 1) which immediately transfers an electron to oxygen generating superoxide anion and the parent paraquat molecule (Bus and Gibson, 1984). Under anaerobic conditions, the paraquat radical is stable (Winterbourn, 1981). Figure 6 shows that lysates from differentiated keratinocytes readily generated the paraquat radical once anaerobic conditions were established. The formation of the paraquat radical was time- and concentration-dependent (Fig. 6 inset and not shown). The presence of the paraquat radical was confirmed by the appearance of a blue-violet color in the reaction mix (Tampo *et al.*, 1999). No major differences were observed in paraquat radical formation between undifferentiated and differentiated keratinocytes (not shown).

Effects of paraquat on oxidative stress in keratinocytes

The oxidation of proteins by ROI is known to be an important marker of cellular oxidative stress (Dean *et al.*, 1997b; Davies, 2005). In both undifferentiated and differentiated keratinocytes, constitutive levels of oxidized proteins were detectable. In particular, two oxidized proteins with molecular masses of 59 and 68 kDa were evident (Fig. 7). Lower levels of proteins with molecular masses of 75 and 97 kDa were also apparent and paraquat treatment of the cells resulted in an increase in oxidation of these proteins. Additionally, a band of oxidized protein at 43 kDa appeared after paraquat treatment in both undifferentiated and differentiated cells.

It is well recognized that oxidative stress upregulates expression of antioxidant enzymes (Franco *et al.*, 1999; Scandalios, 2005). In both undifferentiated and differentiated keratinocytes, paraquat treatment increased mRNA expression of HO-1, Cu,Zn-SOD and catalase approximately 5–8 fold (Fig. 8, upper panel). Paraquat treatment also resulted in increased protein expression of these antioxidants (Fig. 8, lower panel). No major differences in expression of the antioxidants were noted between paraquat-treated undifferentiated and differentiated cells. In contrast, paraquat had no effect on expression of Mn-SOD, GPx-1 or MT-2 (Fig. 8, upper panel). Interestingly, we also found that the differentiation process was associated with increased constitutive expression of HO-1, Cu,Zn-SOD and catalase protein.

The glutathione *S*-transferase (GST) enzymes play a central role in the elimination of oxidized macromolecules and xenobiotics in cells through glutathione conjugation (Hayes *et al.*, 2004). The major cytosolic members of the GST superfamily are the alpha (GSTA), mu (GSTM) and pi (GSTP) families which are important in detoxification of lipid and protein peroxidation products (Hayes and Strange, 1995; Hayes and McLellan, 1999). The three microsomal GST enzymes (mGST1, mGST2 and mGST3) are members of the membrane-associated proteins in the eicosanoid and glutathione metabolism (MAPEG) family of enzymes (Jakobsson *et al.*, 1999; Jakobsson *et al.*, 2000) and are also important in removing oxidation products (Mosialou *et al.*, 1995). We found that mRNA expression of the alpha family of GST's was markedly increased in differentiated and undifferentiated keratinocytes in response to paraquat treatment. Specifically, GSTA1-2 was increased 40–50-fold, while GSTA4 increased 20–25-fold (Fig. 9, left panel). Paraquat also stimulated GSTA3 expression 9–13-fold (Fig. 9A), while GSTP1 levels increased 3–4-fold in both cell types (Fig. 9, right panel). Increases in GSTA1-2, but not in GSTA4, GSTA3 or GSTP1, were significantly greater in differentiated cells when compared to undifferentiated cells. No major changes were observed in GSTM1, mGST1, mGST2 or mGST3 expression following paraquat treatment in either undifferentiated and differentiated cells.

Discussion

The present studies show that paraquat is reduced to a radical in keratinocytes during a redox cycling reaction, and that oxidation of this radical generates superoxide anion and hydrogen peroxide. Moreover, in intact keratinocytes, paraquat redox cycling leads to protein oxidation. These findings are novel and suggest a potential mechanism mediating paraquat-induced injury to the skin. Of particular interest was our observation that paraquat-induced protein oxidation was greater in differentiated keratinocytes, when compared to undifferentiated cells, and that this is associated with increased hydrogen peroxide formation. These results suggest that differentiated keratinocytes may be more susceptible to oxidative stress. This idea is consistent with findings of increased oxidative stress in suprabasal layers of the epidermis following exposure to UVB light (Theile *et al.*, 1999; Sander *et al.*, 2002). In contrast, we noted that generally similar amounts of superoxide anion were generated in undifferentiated and differentiated keratinocytes. It is possible that differentiated cells metabolize superoxide anion more rapidly than undifferentiated cells. This is supported by our findings that differentiated

cells expressed greater constitutive levels of Cu,Zn-SOD. Although differentiated cells also expressed more catalase, this was apparently not sufficient to metabolize hydrogen peroxide during paraquat redox cycling in these cells, when compared to undifferentiated cells. At least four constitutively oxidized proteins with molecular masses of 59, 68, 75 and 97 kDa were identified in the keratinocytes. It is well recognized that cells continuously generate basal levels of superoxide anion and hydrogen peroxide from both mitochondrial and extramitochondrial sources (Darr and Fridovich, 1994), and it is likely that these ROI are responsible for generating the observed oxidized proteins. This is in accord with our findings of enhanced oxidation of these same proteins following paraquat treatment. Paraquat also induced oxidation of an additional 43 kDa protein in both differentiated and undifferentiated keratinocytes. At the present time, the identity of the oxidized target proteins in the cells is not known. Since the 43 kDa protein is selectively oxidized following paraquat treatment, we speculate that it plays a critical role in mediating the biological actions of paraquat.

Previous studies have demonstrated that redox cycling of paraquat occurs via the actions of oxidoreductases including cytochrome P450 reductase and thioredoxin reductase (Day *et al.*, 1999; Gray *et al.*, 2007). These are flavin-containing monooxygenases that are inhibited by DPI. In accord with this, we found that DPI also inhibited paraquat-mediated redox cycling in keratinocyte lysates. However, the redox cycling activity was simultaneously suppressed by dicoumarol, an inhibitor of the FAD-containing enzyme, NAD(P)H quinone oxidoreductase-1 (NQO1). Although these findings suggest that paraquat may redox cycle with this enzyme, this would be surprising since NQO1 catalyzes an obligate two-electron reduction (Chen *et al.*, 2000). It should be noted that dicoumarol also inhibits other enzymes including mitochondrial complexes II, III and IV (Gonzalez-Aragon *et al.*, 2007). Thus, we cannot rule out the possibility that dicoumarol inhibits other DPI-sensitive one electron oxidoreductases in keratinocytes that mediate redox cycling of paraquat.

Increased oxidative stress in cells is associated with altered expression of antioxidant enzymes which function to limit cytotoxicity (Adler *et al.*, 1999; Droge, 2002; Scandalios, 2005). Both undifferentiated and differentiated keratinocytes were found to respond to paraquat-induced oxidative stress by upregulating the expression of several key antioxidant enzymes including Cu,Zn-SOD, HO-1 and catalase. Transgenic mouse studies have shown that antioxidant enzymes such as Cu,Zn-SOD, as well as GPx-1, are required for the prevention of paraquat-induced oxidative damage (de Haan *et al.*, 1998; Van Remmen *et al.*, 2004), and that their overexpression offers protection from injury (Thiruchelvam *et al.*, 2005). Interestingly, we found differential effects of paraquat on expression of Cu,Zn-SOD and Mn-SOD. Thus, while Cu,Zn-SOD was readily induced in the cells following paraquat treatment, Mn-SOD remained unchanged. Similar results have been described in paraquat-treated fibroblasts (Kelner and Bagnell, 1990), and in keratinocytes exposed to UVB (Sasaki *et al.*, 1997). Cu,Zn-SOD and Mn-SOD are known to be regulated by distinct mechanisms (Zelko *et al.*, 2002). Moreover, Cu,Zn-SOD is cytosolic, while Mn-SOD is restricted to the mitochondrial matrix and inner membrane (Fridovich, 1978). Presumably, paraquat generates superoxide anion in the cytosolic compartment of the cells and localized oxidative stress stimulates expression of Cu,Zn-SOD.

Paraquat-induced increases in HO-1 expression were also observed in undifferentiated and differentiated cells. HO-1, like Cu,Zn-SOD, is upregulated in cultured skin and lung cells in response to exposure to oxidants such as ozone (Valacchi *et al.*, 2004), sodium arsenite (Applegate *et al.*, 1991) and UVA (Keyse and Tyrrell, 1990). This is thought to be central in antioxidant defense and is supported by findings that HO-1 knockout mice exhibit increased ROI production and enhanced mortality (Poss and Tonegawa, 1997). As observed with Cu,Zn-SOD and catalase, constitutive expression of HO-1 was increased in differentiated keratinocytes when compared to undifferentiated cells, and this may be important in protecting suprabasal layers of the skin from oxidative stress. Catalase expression was also induced by

paraquat in both undifferentiated and differentiated keratinocytes. Increased catalase expression has been observed in skin following UVA exposure (Fuchs *et al.*, 1989), and catalase overexpression in both cultured keratinocytes and mice provides protection from hydrogen peroxide-induced damage (Chen *et al.*, 2004; Shim *et al.*, 2005), as well as UVB-mediated apoptosis (Rezvani *et al.*, 2006). Increased expression of these important antioxidants is a key adaptive response to protein oxidation as a result of paraquat redox cycling and represents a mechanism to protect keratinocytes against further oxidative stress.

Of particular interest was our finding that paraquat treatment altered expression of several major glutathione *S*-transferase (GST) enzymes. A major function of both cytosolic and microsomal GST enzymes is conjugation of glutathione to oxidized cellular macromolecules in order to facilitate their elimination and limit tissue injury. Although all GST enzymes conjugate glutathione, each GST family has preferred substrates. GSTA enzymes have been shown to break lipid peroxidation chain reactions through the removal of hydroperoxides and aldehydes generated during oxidative stress (Hayes and McLellan, 1999; Yang *et al.*, 2002). This GSTA preference for lipid peroxidation products may explain the striking increases in GSTA1-2 and GSTA4, as well as GSTA3 that we observed in keratinocytes. Our findings are consistent with previous work showing that overexpression of GSTA1 protects against hydrogen peroxide-induced cytotoxicity and DNA damage in retinal pigment cells (Liang *et al.*, 2005). We also noted significantly greater expression of GSTA1-2 in response to paraquat in differentiated keratinocytes, when compared to undifferentiated cells. Genetic polymorphisms in the GSTA1 promoter have been associated with increased cancer incidence (Coles *et al.*, 2001; Sweeney *et al.*, 2003), and these polymorphisms may be involved in regulating GSTA1 gene expression and tumor development. The importance of GSTA4 activity in protection against paraquat-induced oxidative stress has also been noted in GSTA4 null mice (Engle *et al.*, 2004). Higher concentrations of lipid peroxidation products are detected in the livers of these mice after injection of paraquat, and the mice exhibit a greater mortality relative to wild-type controls. The lower induction of GSTP1, and lack of induction of GSTM1 in our cells may be due to the diminished roles that these enzyme families play in the detoxification of lipid peroxidation products (Berhane *et al.*, 1994). Our results are generally similar to reports of changes in GST mRNA expression in lungs from mice treated with paraquat where increases in the GST alpha and pi families were detected (Ruiz-Laguna *et al.*, 2005).

The microsomal GST (mGST) enzymes have been shown to exhibit glutathione peroxidase activity against lipid hydroperoxides that is similar to the cytosolic GSTA enzymes (Mosialou *et al.*, 1995). However, in keratinocytes, expression of these enzymes was not altered by paraquat treatment. The mGSTs also appear to be important in the metabolism of lipid-derived inflammatory mediators (Hayes *et al.*, 2004). Both mGST2 and mGST3 conjugate glutathione to leukotriene A_4 to form leukotriene C_4 (LTC_4) (Jakobsson *et al.*, 1997), while mGST1 co-localizes with leukotriene C_4 synthase, and is inhibited by LTC_4 (Bannenberg *et al.*, 1999). Further studies are necessary to determine if the microsomal and cytosolic GST enzymes are regulated distinctly, and to elucidate their role in protecting cells from oxidative stress.

Our data show that paraquat readily induced oxidative stress in keratinocytes. Antioxidant therapy involving the administration of SOD or N-acetylcysteine (NAc) has been proposed as a potential treatment for paraquat poisoning. This approach, however, has met with mixed results. While initial studies suggested that NAc and Cu,Zn-SOD increased the survival of paraquat-treated animals (Yeh *et al.*, 2006), subsequent work demonstrated that the protective effects of SOD were only evident when it was used in combination with Mn-SOD and glutathione (GSH) (Paller and Eaton, 1995). In the same study, Cu,Zn-SOD treatment alone enhanced oxidative injury, primarily due to the reactivity of the copper ions. In recent *in vivo* experiments, synthetic SOD analogs were shown to prevent paraquat-induced pulmonary

oxidative damage without causing toxicity in mice (Day and Crapo, 1996). In mouse skin, topical application of antioxidant formulations including inhibitors of superoxide anion or alpha- and beta-carotenes reduced markers of oxidative stress caused by exposure to phorbol esters (Nakamura *et al.*, 1998) or croton oil (Kim-Jun, 1993). At the present time, the use of antioxidants orally or topically for the treatment of paraquat toxicity is promising but requires additional studies to identify agents that penetrate the skin and retain biological activity.

In summary, we have shown that paraquat induces oxidative stress in primary cultures of undifferentiated and differentiated mouse keratinocytes by producing ROI via NADPH-dependent redox cycling. This leads to increased protein oxidation, particularly in differentiated cells, as well as upregulation of critical antioxidant enzymes including Cu,Zn-SOD, catalase, HO-1, GSTA1-2, GSTA3, GSTA4 and GSTP1. At the present time, the precise role of each of these antioxidants in the response of the skin to oxidative stress is unknown. The role of differentiation in regulating antioxidant enzyme expression, as well as in determining of how this process controls the responses of the skin to oxidative stress requires further investigation for a more complete understanding of the dermal toxicity of paraquat.

Acknowledgements

This work was supported in part by National Institutes of Health grants CA100994, CA093798, GM034310, ES004738, ES005022 and by NJ State Commission on Cancer Research fellowship 05-2413-CCR-E0. This work was also funded in part by the National Institutes of Health CounterACT Program through the National Institute of Arthritis and Musculoskeletal and Skin Diseases (award #U54AR055073). Its contents are solely the responsibility of the authors and do not necessarily represent the official views of the federal government.

Abbreviations

DPI, diphenyleneiodonium
GST, glutathione *S*-transferase
GSTA, GST alpha
GSTM, GST mu
GSTP, GST pi
GPx-1, glutathione peroxidase-1
HO-1, heme oxygenase-1
Cu,Zn-SOD, copper-zinc superoxide dismutase
Mn-SOD, manganese superoxide dismutase
MT-2, metallothionein-2
NQO1, NAD(P)H quinone oxidoreductase-1
PBS, phosphate-buffered saline

References

Adler V, Yin Z, Tew KD, Ronai Z. Role of redox potential and reactive oxygen species in stress signaling. Oncogene 1999;18:6104–6111. [PubMed: 10557101]

Anderson KD, Scerri GV. A case of multiple skin cancers after occupational exposure to pesticides. Br J Dermatol 2003;149:1088–1089. [PubMed: 14632830]

Applegate LA, Luscher P, Tyrrell RM. Induction of heme oxygenase: a general response to oxidant stress in cultured mammalian cells. Cancer Res 1991;51:974–978. [PubMed: 1988141]

Asher G, Dym O, Tsvetkov P, Adler J, Shaul Y. The crystal structure of NAD(P)H quinone oxidoreductase 1 in complex with its potent inhibitor dicoumarol. Biochemistry 2006;45:6372–6378. [PubMed: 16700548]

Bannenberg G, Dahlen SE, Luijerink M, Lundqvist G, Morgenstern R. Leukotriene C_4 is a tight-binding inhibitor of microsomal glutathione transferase-1. Effects of leukotriene pathway modifiers. J Biol Chem 1999;274:1994–1999. [PubMed: 9890956]

Berhane K, Widersten M, Engstrom A, Kozarich JW, Mannervik B. Detoxification of base propenals and other alpha, beta-unsaturated aldehyde products of radical reactions and lipid peroxidation by human glutathione transferases. Proc. Natl. Acad. Sci. USA 1994;91:1480–1484. [PubMed: 8108434]

Bonneh-Barkay D, Reaney SH, Langston WJ, Di Monte DA. Redox cycling of the herbicide paraquat in microglial cultures. Brain Res Mol Brain Res 2005;134:52–56. [PubMed: 15790529]

Bus JS, Aust SD, Gibson JE. Superoxide- and singlet oxygen-catalyzed lipid peroxidation as a possible mechanism for paraquat (methyl viologen) toxicity. Biochem Biophys Res Commun 1974;58:749–755. [PubMed: 4365647]

Bus JS, Cagen SZ, Olgaard M, Gibson JE. A mechanism of paraquat toxicity in mice and rats. Toxicol Appl Pharmacol 1976;35:501–513. [PubMed: 1265764]

Bus JS, Gibson JE. Mechanisms of superoxide radical-mediated toxicity. J Toxicol Clin Toxicol 1982;19:689–697. [PubMed: 6298444]

Bus JS, Gibson JE. Paraquat: model for oxidant-initiated toxicity. Environ Health Perspect 1984;55:37–46. [PubMed: 6329674]

Chen S, Wu K, Knox R. Structure-function studies of DT-diaphorase (NQO1) and NRH:quinone oxidoreductase (NQO2). Free Radic Biol Med 2000;29:276–284. [PubMed: 11035256]

Chen X, Liang H, Van Remmen H, Vijg J, Richardson A. Catalase transgenic mice: characterization and sensitivity to oxidative stress. Arch Biochem Biophys 2004;422:197–210. [PubMed: 14759608]

Chevion M, Berenshtein E, Stadtman ER. Human studies related to protein oxidation: protein carbonyl content as a marker of damage. Free Radic Res 2000;33:S99–S108. [PubMed: 11191280]

Coles BF, Morel F, Rauch C, Huber WW, Yang M, Teitel CH, Green B, Lang NP, Kadlubar FF. Effect of polymorphism in the human glutathione S-transferase A1 promoter on hepatic GSTA1 and GSTA2 expression. Pharmacogenetics 2001;11:663–669. [PubMed: 11692074]

Coyle P, Philcox JC, Carey LC, Rofe AM. Metallothionein: the multipurpose protein. Cell Mol Life Sci 2002;59:627–647. [PubMed: 12022471]

Dalle-Donne I, Aldini G, Carini M, Colombo R, Rossi R, Milzani A. Protein carbonylation, cellular dysfunction, and disease progression. J Cell. Mol. Med 2006;10:389–406. [PubMed: 16796807]

Darr D, Fridovich I. Free radicals in cutaneous biology. J Invest Dermatol 1994;102:671–675. [PubMed: 8176246]

Davies MJ. The oxidative environment and protein damage. Biochem Biophys Acta 2005;1703:93–109. [PubMed: 15680218]

Day BJ, Crapo JD. A metalloporphyrin superoxide dismutase mimetic protects against paraquat-induced lung injury. Toxicol Appl Pharmacol 1996;140:94–100. [PubMed: 8806874]

Day BJ, Patel M, Calavetta L, Chang LY, Stamler JS. A mechanism of paraquat toxicity involving nitric oxide synthase. PNAS USA 1999;26:12760–12765. [PubMed: 10535996]

de Haan JB, Bladier C, Griffiths P, Kelner M, O'Shea RD, Cheung NS, Bronson RT, Silvestro MJ, Wild S, Zheng SS, Beart PM, Hertzog PJ, Kola I. Mice with a homozygous null mutation for the most abundant glutathione peroxidase, Gpx1, show increased susceptibility to the oxidative stress-inducing agents paraquat and hydrogen peroxide. J Biol Chem 1998;273:22528–22536. [PubMed: 9712879]

Dean RT, Fu S, Stocker R, Davies MJ. Biochemistry and pathology of radical-mediated protein oxidation. Biochem J 1997;324:1–18. [PubMed: 9164834]

Droge W. Free radicals in the physiological control of cell function. Physiol Rev 2002;82:47–95. [PubMed: 11773609]

Engle MR, Singh SP, Czernik PJ, Gaddy D, Montague DC, Ceci JD, Yang Y, Awasthi S, Awasthi YC, Zimniak P. Physiological role of mGSTA4-4, a glutathione *S*-transferase metabolizing 4-hydroxynonenal: generation and analysis of *mGsta4* null mouse. Toxicol Appl Pharmacol 2004;194:296–308. [PubMed: 14761685]

Franco AA, Odom RS, Rando TA. Regulation of antioxidant enzyme gene expression in response to oxidative stress and during differentiation of mouse skeletal muscle. Free Radic Biol Med 1999;27:1122–1132. [PubMed: 10569645]

Fridovich I. The biology of oxygen radicals. Science 1978;201:875–880. [PubMed: 210504]

Fuchs J, Huflejt ME, Rothfuss LM, Wilson DS, Carcamo G, Packer L. Acute effects of near ultraviolet light and visible light on the cutaneous antioxidant system. Photochem Photobiol 1989;50:739–744. [PubMed: 2626489]

Gonzalez-Aragon D, Ariza J, Villalba JM. Dicoumarol impairs mitochondrial electron transport and pyrimidine biosynthesis in human myeloid leukemia HL-60 cells. Biochem Pharmacol 2007;73:427–439. [PubMed: 17123468]

Gray JP, Heck DE, Mishin V, Smith PJ, Hong J-Y, Thiruchelvam M, Cory-Slechta DA, Laskin DL, Laskin JD. Paraquat increases cyanide-insensitive respiration in murine lung epithelial cells by activating an NAD(P)H:paraquat oxidoreductase. J Biol Chem 2007;282:7939–7949. [PubMed: 17229725]

Hager B, Bickenbach JR, Fleckman P. Long-term culture of murine epidermal keratinocytes. J Invest Dermatol 1999;112:971–976. [PubMed: 10383747]

Hayes JD, Flanagan JU, Jowsey IR. Glutathione transferases. Annu Rev Pharmacol Toxicol 2004;45:51–88. [PubMed: 15822171]

Hayes JD, McLellan LI. Glutathione and glutathione-dependent enzymes represent a co-ordinately regulated defense against oxidative stress. Free Radic Res 1999b;31:273–300. [PubMed: 10517533]

Hayes JD, Strange RC. Potential contribution of the glutathione S-transferase supergene family to resistance to oxidative stress. Free Radic Res 1995;22:193–207. [PubMed: 7757196]

Jakobsson P-J, Morgenstern R, Mancini J, Ford-Hutchinson A, Persson B. Common structural features of *MAPEG*-a widespread superfamily of membrane associated proteins with highly divergent functions in eicosanoid and glutathione metabolism. Protein Sci 1999;8:689–692. [PubMed: 10091672]

Jakobsson P-J, Morgenstern R, Mancini J, Ford-Hutchinson A, Persson B. Membrane-associated proteins in eicosanoid and glutathione metabolism (MAPEG). Am. J. Resp. Crit. Care Med 2000;161:S20–S24. [PubMed: 10673221]

Jakobsson PJ, Mancini JA, Riendeau D, Ford-Hutchinson AW. Identification and characterization of a novel microsomal enzyme with glutathione-dependent transferase and peroxidase activities. J Biol Chem 1997;272:22934–22939. [PubMed: 9278457]

Jee SH, Kuo HW, Su WP, Chang CH, Sun CC, Wang JD. Photodamage and skin cancer among paraquat workers. Int J Dermatol 1995;34:466–469. [PubMed: 7591408]

Kelner MJ, Bagnell R. Alteration of endogenous glutathione peroxidase, manganese superoxide dismutase, and glutathione transferase activity in cells transfected with a copper-zinc superoxide dismutase expression vector. Explanation for variations in paraquat resistance. J Biol Chem 1990;265:10872–10875. [PubMed: 2358446]

Keyse SH, Tyrrell RM. Induction of the heme oxygenase gene in human skin fibroblasts by hydrogen peroxide and UVA (365 nm) radiation: evidence for the involvement of the hydroxyl radical. Carcinogenesis 1990;11:787–791. [PubMed: 2159388]

Kim-Jun H. Inhibitory effects of alpha- and beta-carotene on croton oil-induced or enzymatic lipid peroxidation and hydroperoxide production in mouse skin epidermis. Int J Biochem 1993;25:911–915. [PubMed: 8344446]

Kishi T, Takahashi T, Mizobuchi S, Mori K, Okamoto T. Effect of dicumarol, a Nad(P)h: quinone acceptor oxidoreductase 1 (DT-diaphorase) inhibitor on ubiquinone redox cycling in cultured rat hepatocytes. Free Radic Res 2002;36:413–419. [PubMed: 12069105]

Krall J, Bagley AC, Mullenbach GT, Hallewell RA, Lynch RE. Superoxide mediates the toxicity of paraquat for cultured mammalian cells. J Biol Chem 1988;263:1910–1914. [PubMed: 2828357]

Levine RL. Carbonyl modified proteins in cellular regulation, aging, and disease. Free Radic Biol Med 2002;32:790–796. [PubMed: 11978480]

Liang F-Q, Alssadi R, Morehead P, Awasthi YC, Godley BF. Enhanced expression of glutathione-S-transferase A1-1 protects against oxidative stress in human retinal pigment epithelial cells. Exp Eye Res 2005;80:113–119. [PubMed: 15652532]

Maines MD, Panahian N. The heme oxygenase system and cellular defense mechanisms. Do HO-1 and HO-2 have different functions? Adv Exp Med Biol 2001;502:249–272. [PubMed: 11950143]

Michaelis L, Hill ES. The viologen indicators. J Gen Physiol 1933;16:859–874.

Mosialou E, Oiemonte F, Andersson C, Vos RM, van Bladeren PJ, Morgenstern R. Microsomal glutathione transferase: lipid-derived substrates and lipid dependence. Arch Biochem Biophys 1995;320:210–216. [PubMed: 7625826]

Nakamura Y, Murakami A, Ohto Y, Torikai K, Tanaka T, Ohigashi H. Suppression of tumor promoter-induced oxidative stress and inflammatory responses in mouse skin by a superoxide generation inhibitor 1'-acetoxychavicol acetate. Cancer Res 1998;58:4832–4839. [PubMed: 9809987]

O'Donnell VB, Tew DG, Jones OTG, England PJ. Studies on the inhibitory mechanisms of iodonium compounds with special reference to neutrophil NADPH oxidase. Biochem J 1993;290:41–49. [PubMed: 8439298]

Paller MS, Eaton JW. Hazards of antioxidant combinations containing superoxide dismutase. Free Radic Biol Med 1995;18:883–890. [PubMed: 7797096]

Poss KD, Tonegawa S. Reduced stress defense in heme oxygenase 1-deficient cells. Proc Natl Acad Sci U S A 1997;94:10925–10930. [PubMed: 9380736]

Rezvani HR, Mazurier F, Cario-Andre M, Pain C, Ged C, Taieb A, de Verneuil H. Protective effects of catalase overexpression on UVB-induced apoptosis in normal human keratinocytes. J Biol Chem 2006;281:17999–18007. [PubMed: 16644728]

Riganti C, Gazzano E, Polimeni M, Costamagna C, Bosia A, Ghigo D. Diphenyleneiodonium inhibits the cell redox metabolism and induces oxidative stress. J Biol Chem 2004;279:47726–47731. [PubMed: 15358777]

Ruiz-Laguna J, Abril N, Prieto-Alamo MJ, Lopez-Barea J, Puyeo C. Tissue, species, and environmental differences in absolute quantities of murine mRNAs coding for alpha, mu, omega, pi and theta glutathione *S*-transferases. Gene Exp 2005;12:165–176.

Sander CS, Chang H, Salzmann S, Muller CS, Ekanayake-Mudiyanselage S, Elsner P, Thiele JJ. Photoaging is associated with protein oxidation in human skin *in vivo*. J Invest Dermatol 2002;118:618–625. [PubMed: 11918707]

Sasaki H, Akamatsu H, Horio T. Effects of a single exposure to UVB radiation on the activities and protein levels of copper-zinc and manganese superoxide dismutase in cultured human keratinocytes. Photochem Photobiol 1997;65:707–713. [PubMed: 9114748]

Scandalios JG. Oxidative stress: molecular perception and transduction of signals triggering antioxidant defenses. Braz J Med Biol Res 2005;38:995–1014. [PubMed: 16007271]

Shim JH, Cho KJ, Lee RA, Kim SH, Myung PK, Choe YK, Yoon DY. E7-expressing HaCaT keratinocyte cells are resistant to oxidative stress-induced cell death via the induction of catalase. Proteomics 2005;5:2112–2122. [PubMed: 15852342]

Stadtman ER. Oxidation of free amino acids and amino acid residues in proteins by radiolysis and metal-catalyzed reactions. Ann. Rev. Biochem 1993;62:797. [PubMed: 8352601]

Sweeney C, Ambrosone CB, Joseph L, Stone A, Hutchins LF, Kadlubar FF, Coles BF. Association between a glutathione S-transferase A1 promoter polymorphism and survival after breast cancer treatment. Int J Cancer 2003;103:810–814. [PubMed: 12516103]

Tampo Y, Tsukamoto M, Yonaha M. Superoxide production from paraquat evoked by exogenous NADPH in pulmonary endothelial cells. Free Radic Biol Med 1999;27:588–595. [PubMed: 10490279]

Theile JJ, Hseih SS, Briviba K, Sies H. Protein oxidation in human stratum corneum: susceptibility of keratins to oxidation in vitro and presence of a keratin oxidation gradient in vivo. J Invest Dermatol 1999;113:335–339. [PubMed: 10469330]

Thiele JJ, Traber MG, Tsang K, Cross CE, Packer L. In vivo exposure of ozone depletes vitamins C and E and induces lipid peroxidation in epidermal layers of murine skin. Free Radic Biol Med 1997;23:385–391. [PubMed: 9214574]

Thiruchelvam M, Prokopenko O, Cory-Slechta DA, Richfield EK, Buckley B, Mironitchenko O. Overexpression of superoxide dismutase or glutathione peroxidase protects against the paraquat + maneb-induced Parkinson disease phenotype. J. Biol. Chem 2005;280:22530–22539. [PubMed: 15824117]

Tomita M. Comparison of one-electron reduction activity against the bipyridylium herbicides, paraquat and diquat, in microsomal and mitochondrial fractions of liver, lung and kidney (in vitro). Biochem Pharmacol 1991;42:303–309. [PubMed: 1650209]

Trouba KJ, Hamadeh HK, Amin RP, Germolec DR. Oxidative stress and its role in skin disease. Antiox Redox Signal 2002;4:665–673.

Valacchi G, Pagnin E, Corbacho AM, Olano E, Davis PA, Packer L, Cross CE. In vivo ozone exposure induces antioxidant/stress-related responses to murine lung and skin. Free Radic Biol Med 2004;36:673–681. [PubMed: 14980710]

Van Remmen H, Qi W, Sabia M, Freeman G, Estlack L, Yang H, Mao Guo Z, Huang TT, Strong R, Lee S, Epstein CJ, Richardson A. Multiple deficiencies in antioxidant enzymes in mice result in a compound increase in sensitivity to oxidative stress. Free Radic Biol Med 2004;36:1625–1634. [PubMed: 15182862]

Vetrano AM, Heck DE, Mariano TM, Mishin V, Laskin DL, Laskin JD. Characterization of the oxidase activity in mammalian catalase. J Biol Chem 2005;280:35372–35381. [PubMed: 16079130]

Vilaplana J, Azon A, Romaguera C, Lecha M. Phototoxic contact dermatitis with toxic hepatitis due to the percutaneous absorption of paraquat. Contact Dermatitis 1993;29:163–164. [PubMed: 8222639]

Wang JD, Li WE, Hu FC, Hu KH. Occupational risk and the development of premalignant skin lesions among paraquat manufacturers. Br J Ind Med 1987;44:196–200. [PubMed: 3493801]

Winterbourn CC. Production of hydroxyl radicals from paraquat radicals and H_2O_2. FEBS Lett 1981;128:339–342. [PubMed: 6894903]

Yang Y, Sharma R, Zimniak P, Awasthi YC. Role of alpha class glutathione S-transferases as antioxidant enzymes in rodent tissues. Toxicol Appl Pharmacol 2002;182:105–115. [PubMed: 12140174]

Yeh ST, Gue HR, Su YS, Lin HJ, Hou CC, Chen HM, Chang MC, Wang YJ. Protective effects of N-acetylcysteine treatment post acute paraquat intoxication in rats and human lung epithelial cells. Toxicology 2006;223:181–190. [PubMed: 16713667]

Yu BP. Cellular defenses against damage from reactive oxygen species. Physiol Rev 1994;74:139–162. [PubMed: 8295932]

Yuspa SH, Hennings H, Tucker RW, Jaken S, Kilkenny AE, Roop DR. Signal transduction for proliferation and differentiation in keratinocytes. Ann N Y Acad Sci 1988;548:191–196. [PubMed: 2470295]

Yuspa SH, Kilkenny AE, Steinert PM, Roopq DR. Expression of murine epidermal differentiation markers is tightly regulated by restricted extracellular calcium concentrations in vitro. J Cell Biol 1989;109:1207–1217. [PubMed: 2475508]

Zelko IN, Mariani TJ, Folz RJ. Superoxide dismutase multigene family: a comparison of the CuZn-SOD (SOD1), Mn-SOD (SOD2), and EC-SOD (SOD3) gene structures, evolution, and expression. Free Radic Biol Med 2002;33:337–349. [PubMed: 12126755]

Zhao H, Joseph J, Fales HM, Sokoloski EA, Levine RL, Vasquez-Vivar J, Kalyanaraman B. Detection and characterization of the product of hydroethidine and intracellular superoxide by HPLC and limitations of fluorescence. Proc Natl Acad Sci USA 2005;102:5727–5732. [PubMed: 15824309]

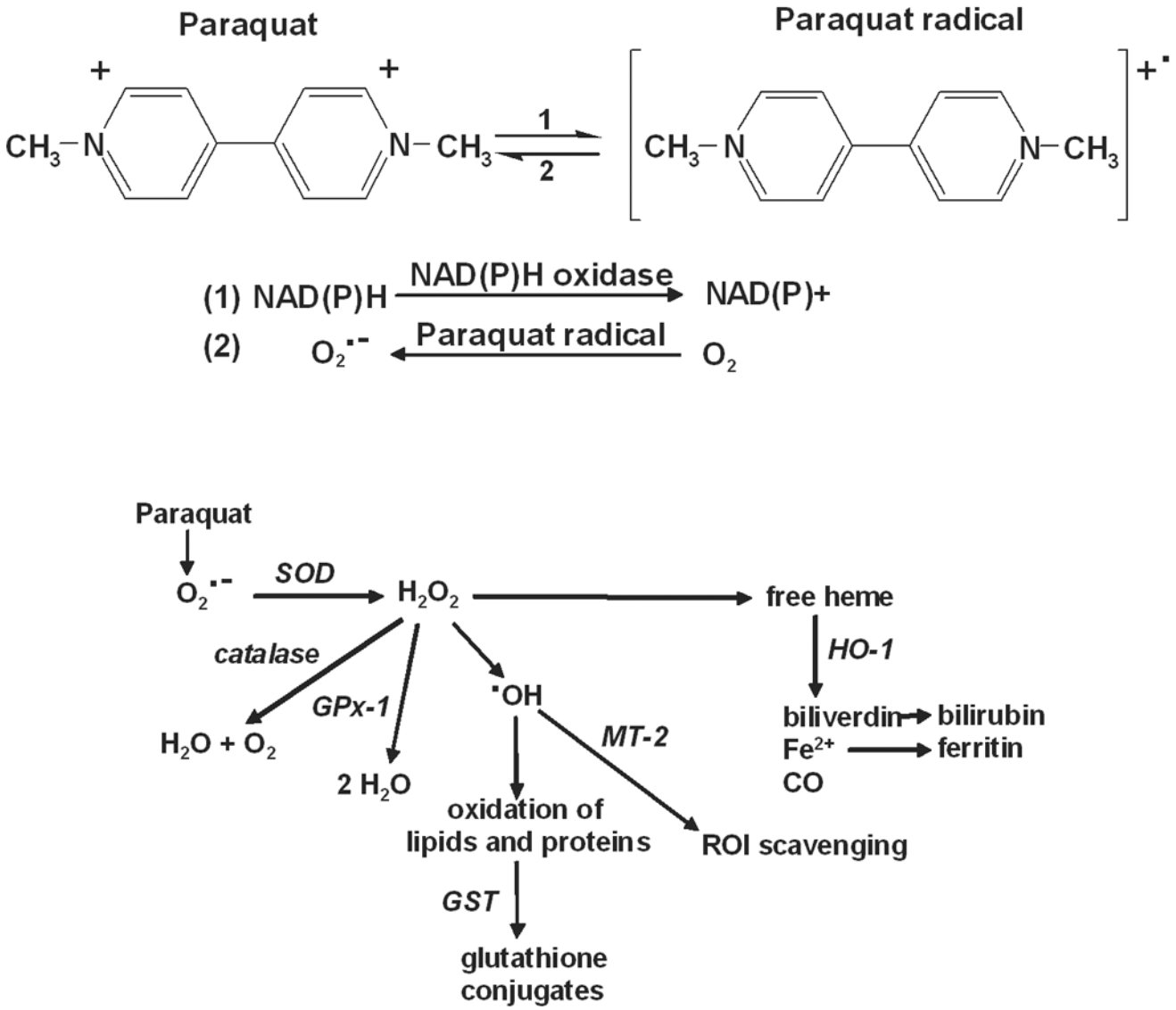

Figure 1. Summary of paraquat redox cycling and detoxification of ROI by cellular antioxidants

Upper panel: Paraquat redox cycling reactions. Paraquat undergoes a one electron reduction to the paraquat radical via the oxidation of NAD(P)H to NAD(P)$^+$ by NAD(P)H oxidase (Reaction 1). The paraquat radical is then immediately oxidized to the parent compound with the transfer of an electron to molecular oxygen, forming superoxide anion (Reaction 2). *Lower panel*: Detoxification of ROI by enzymatic antioxidants. Superoxide anion is metabolized to hydrogen peroxide by SOD. Hydrogen peroxide is detoxified by catalase and/or various peroxidases including GPx-1. Hydrogen peroxide has been implicated in the mobilization of heme, an oxidizing agent, which is then degraded by heme oxygenases including HO-1 to biliverdin, ferric iron and carbon monoxide. Biliverdin is further metabolized to bilirubin and ferric iron is removed through sequestration by ferritin. In the presence of transition metals such as iron or copper, hydrogen peroxide can also be converted to hydroxyl radicals. The zinc-mediated free radical scavenging function of MT-2 serves as a mechanism for removal of hydroxyl radicals. Oxidized proteins and lipids can be conjugated with glutathione by the GST enzymes to facilitate cellular elimination.

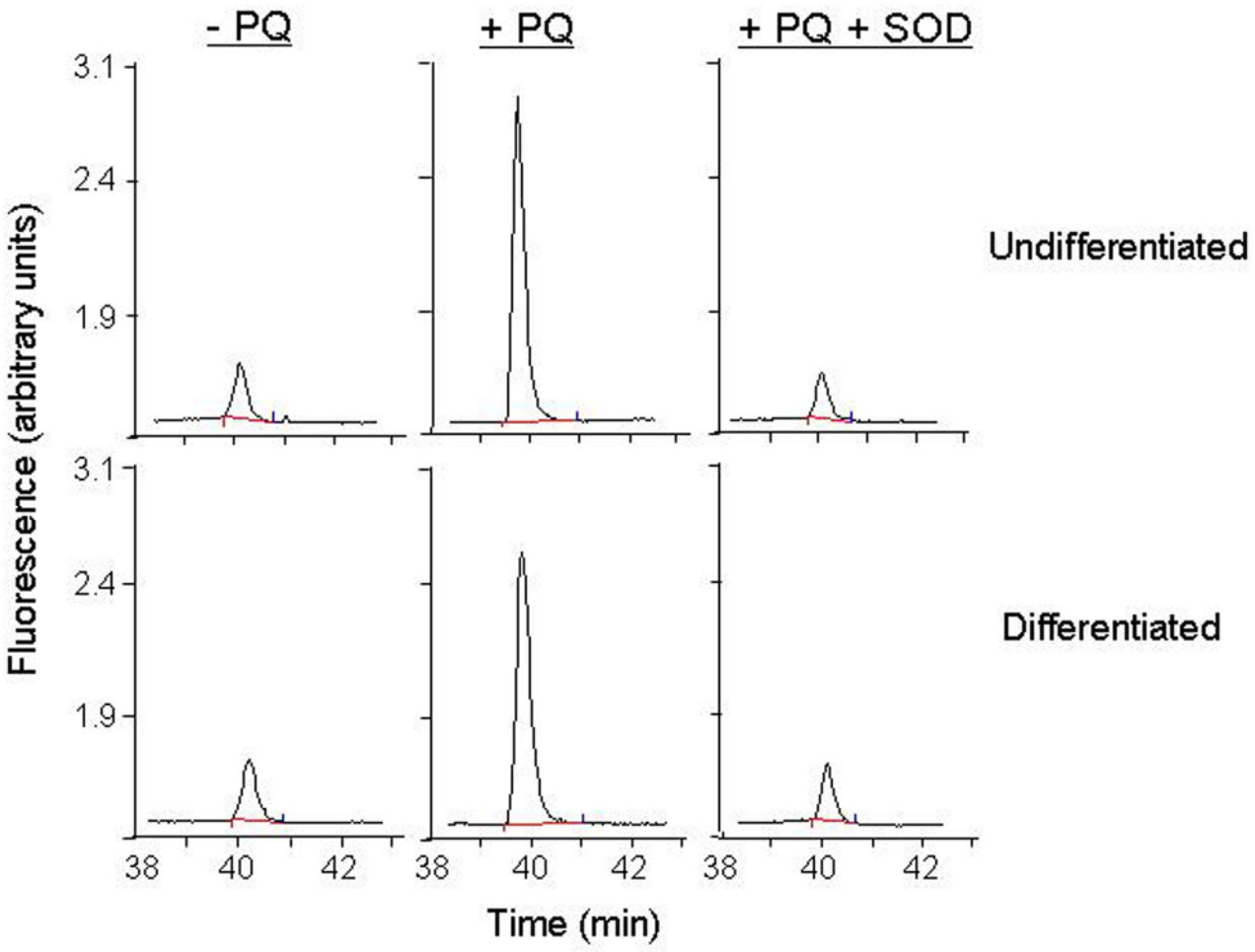

Figure 2. Paraquat redox cycling leads to the production of superoxide anion

Superoxide anion generation was assayed by the formation of 2-hydroxyethidium from dihydroethidine using HPLC. Reaction mixtures contained lysates from undifferentiated and differentiated (130 μg/μl protein), paraquat (100 μM), NADPH (500 μM) and dihydroethidine (40 μM). After one hr at 37°C, 2-hydroxyethidium was extracted and analyzed by HPLC. In some reaction mixes, Cu,Zn-SOD (350 U/ml) was added to confirm that the 2-hydroxyethidium peak was due to superoxide anion production.

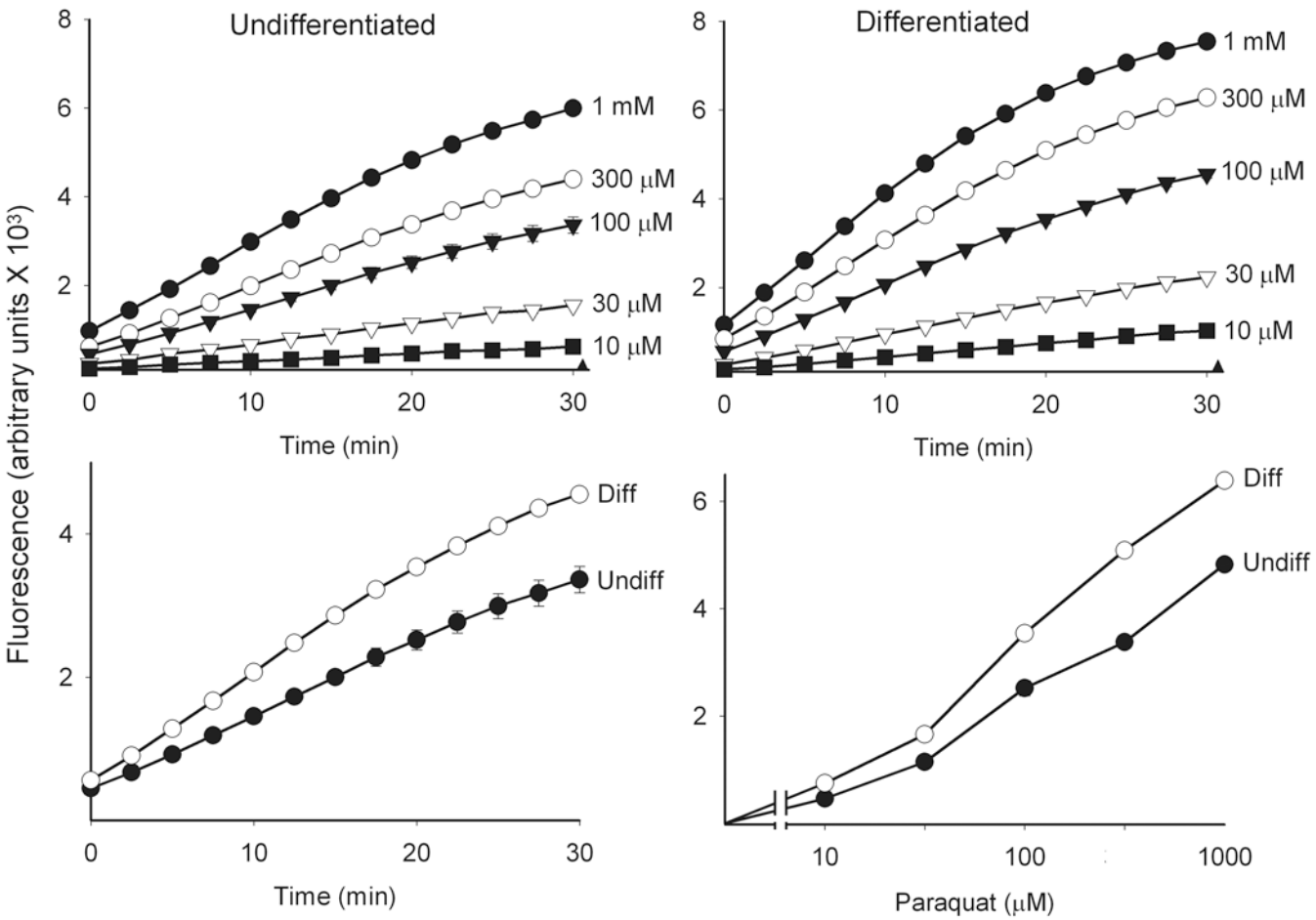

Figure 3. Redox cycling of paraquat by keratinocytes

Paraquat redox cycling was quantified by the formation of hydrogen peroxide in cell lysates as described in the Methods section. Reaction mixtures contained cell lysates (130 μg/μl protein), 500 μM NADPH and paraquat at the indicated concentrations and were run in triplicate. Data are presented as the mean ± SE. Background fluorescence (closed triangles) was subtracted from all values. *Upper panels*: Effects of increasing concentrations of paraquat on hydrogen peroxide formation in lysates from undifferentiated and differentiated keratinocytes. *Lower left panel*: Comparison of paraquat (100 μM) induced hydrogen peroxide formation in lysates from undifferentiated and differentiated cells. *Lower right panel*: Concentration-dependent increase in hydrogen peroxide formation in lysates from undifferentiated and differentiated cells. Assays were run for 30 min.

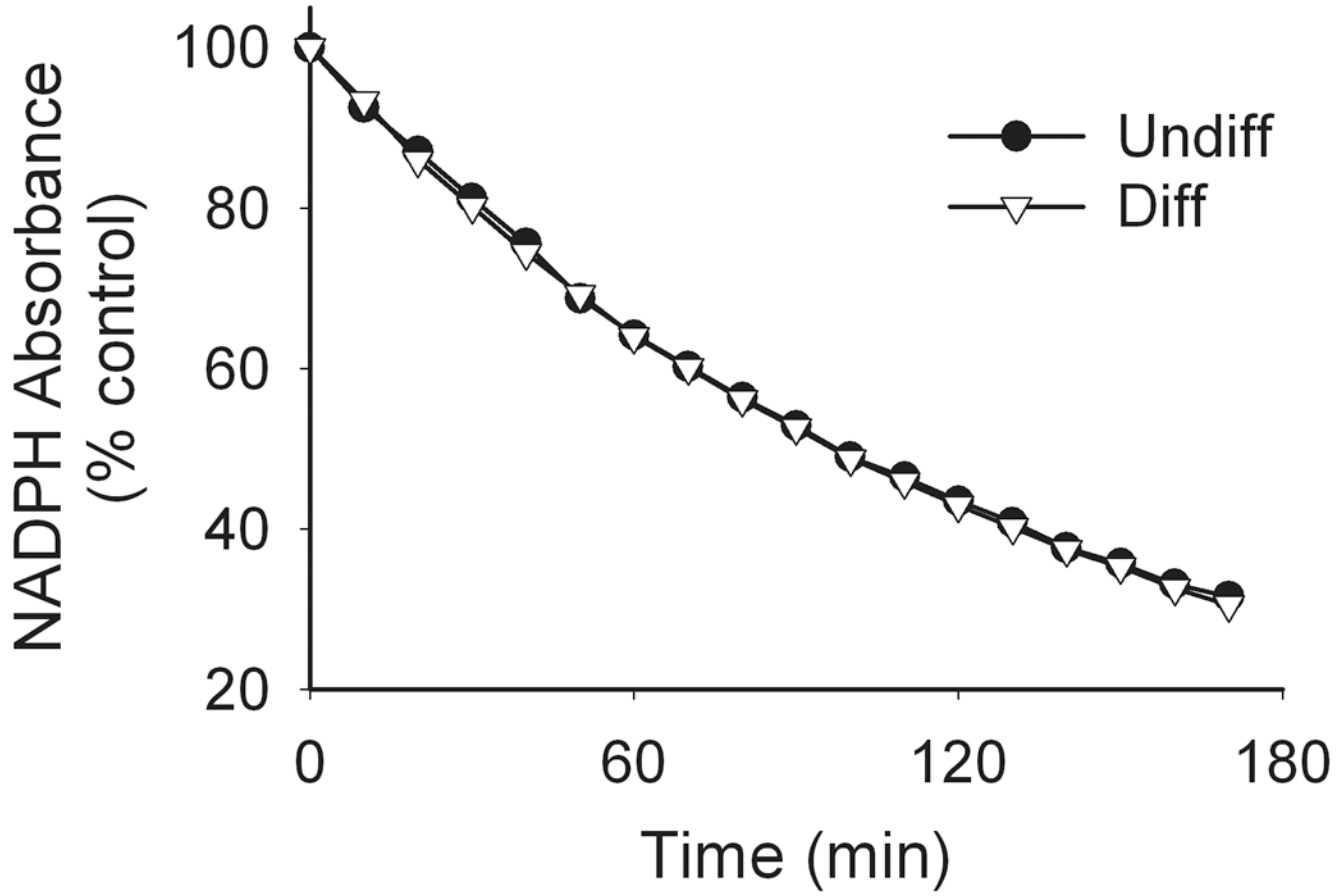

Figure 4. Effects of paraquat on NADPH metabolism

Reaction mixtures contained cell lysates (130 μg/μl protein), 100 μM paraquat and 100 μM NADPH in a 1 ml cuvette. NADPH metabolism was assayed by monitoring changes in absorbance at 340 nm and were recorded every 2.5 min for 3 h using a UV/VIS spectrophotometer. Data are presented as percent of control. Circles, undifferentiated (undiff) cells; triangles, differentiated (diff) cells.

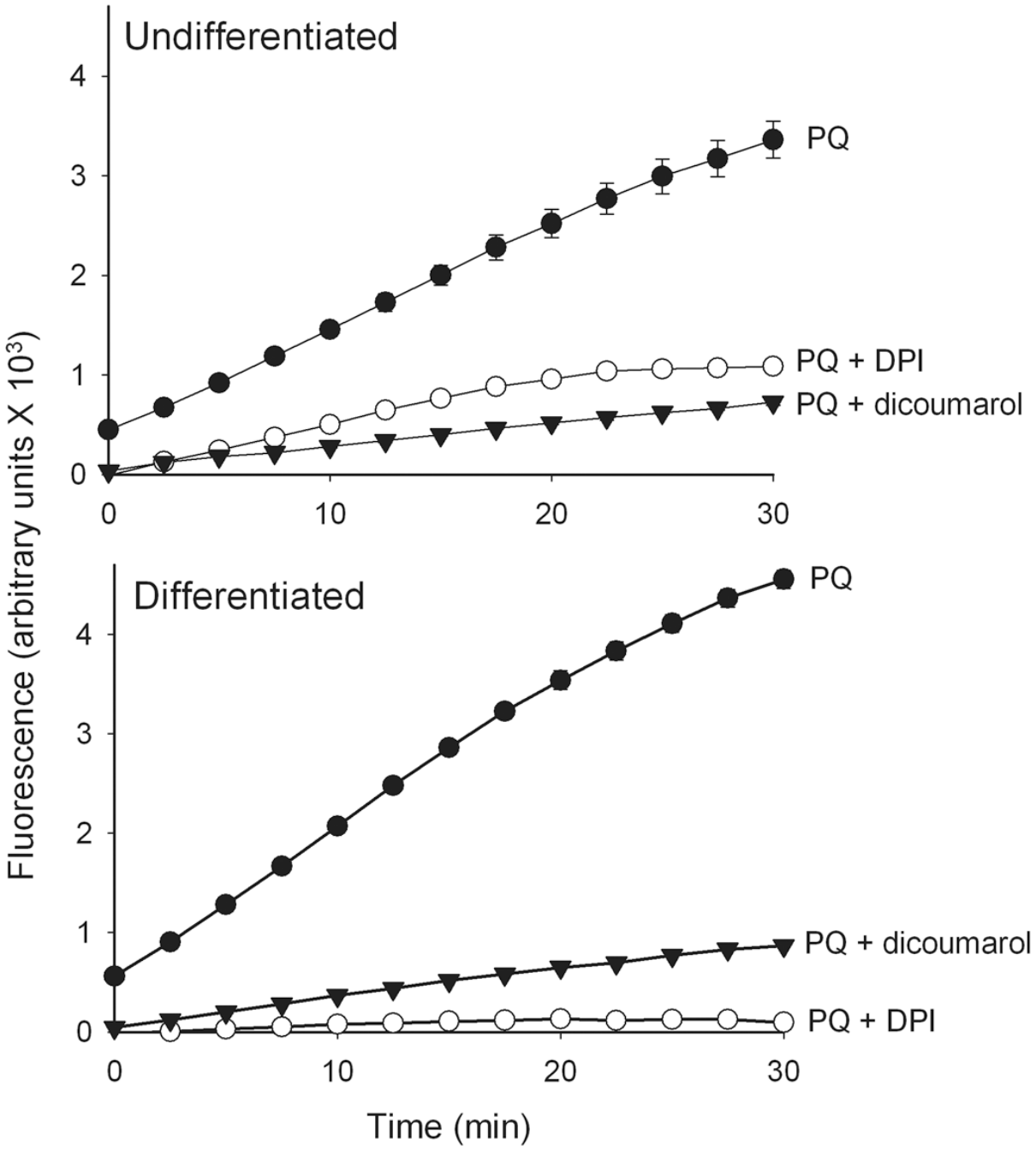

Figure 5. Effects of inhibitors on paraquat redox cycling

Redox cycling of paraquat in keratinocyte lysates was quantified by the production of hydrogen peroxide using the Amplex Red reaction. Enzyme reactions contained lysates (130 μg/μl protein) from undifferentiated and differentiated cells, 100 μM paraquat (PQ) and 500 μM NADPH and were run in the presence and absence of dicoumarol (100 μM) or DPI (10 μM) and were run in triplicate. Data are presented as the mean ± SE. Background fluorescence was subtracted from all values.

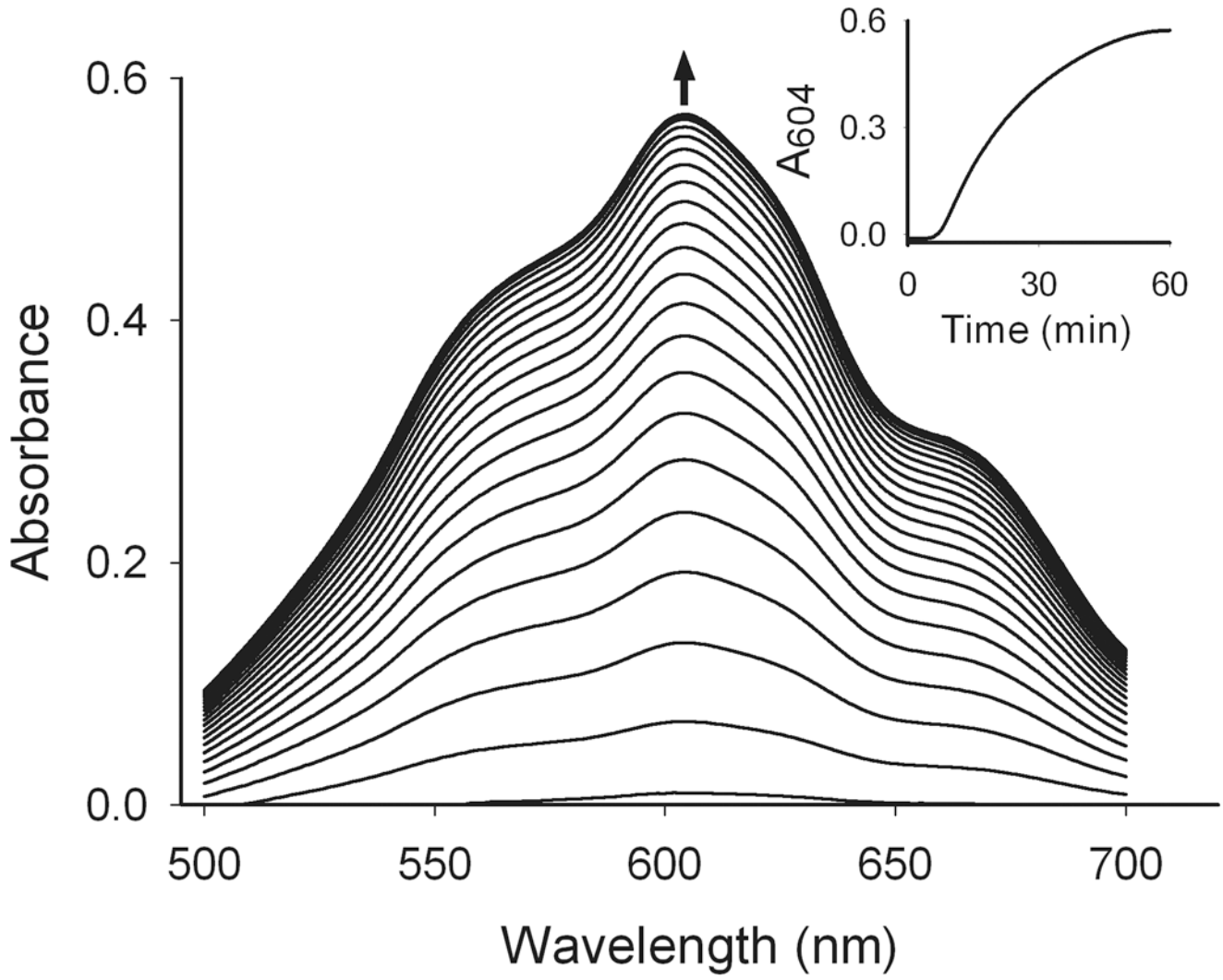

Figure 6. Generation of paraquat radicals

Paraquat metabolism was assayed in reaction mixtures containing cell lysates from undifferentiated keratinocytes (130 μg/μl protein), paraquat (500 μM) and NADPH (3 mM) in sealed cuvettes placed in a UV/VIS spectrophotometer. After 120 min, anaerobic conditions were established and readings were recorded every 2.5 min. The paraquat radical has a peak absorbance peak of 604 nm (Tampo *et al.*, 1999). The inset shows the formation of the paraquat radical over time.

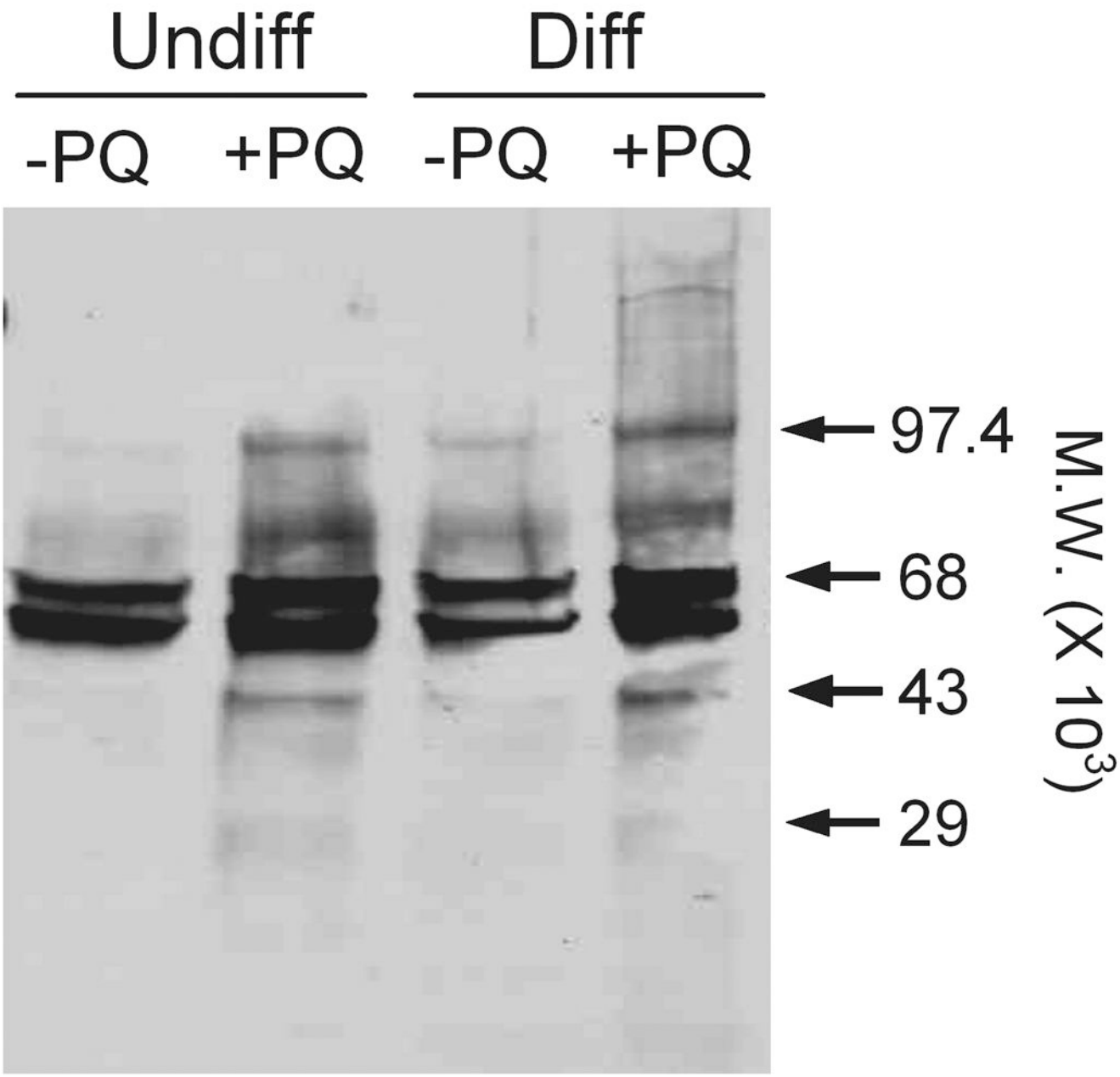

Figure 7. Cellular oxidative stress in paraquat-treated keratinocytes

Undifferentiated (Undiff) and differentiated (Diff) keratinocytes were incubated in growth medium in the absence and presence of 100 μM paraquat (PQ). After 24 h, cell lysates were prepared and carbonyl groups on protein side chains were derivatized using 2,4-dinitrophenylhydrazine. The samples were then separated on SDS-polyacrylamide gels and protein oxidation quantified by Western blotting using an antibody to derivatized carbonyl groups as described in the Methods section. Loading of equal amounts of protein was confirmed by silver staining of the gel.

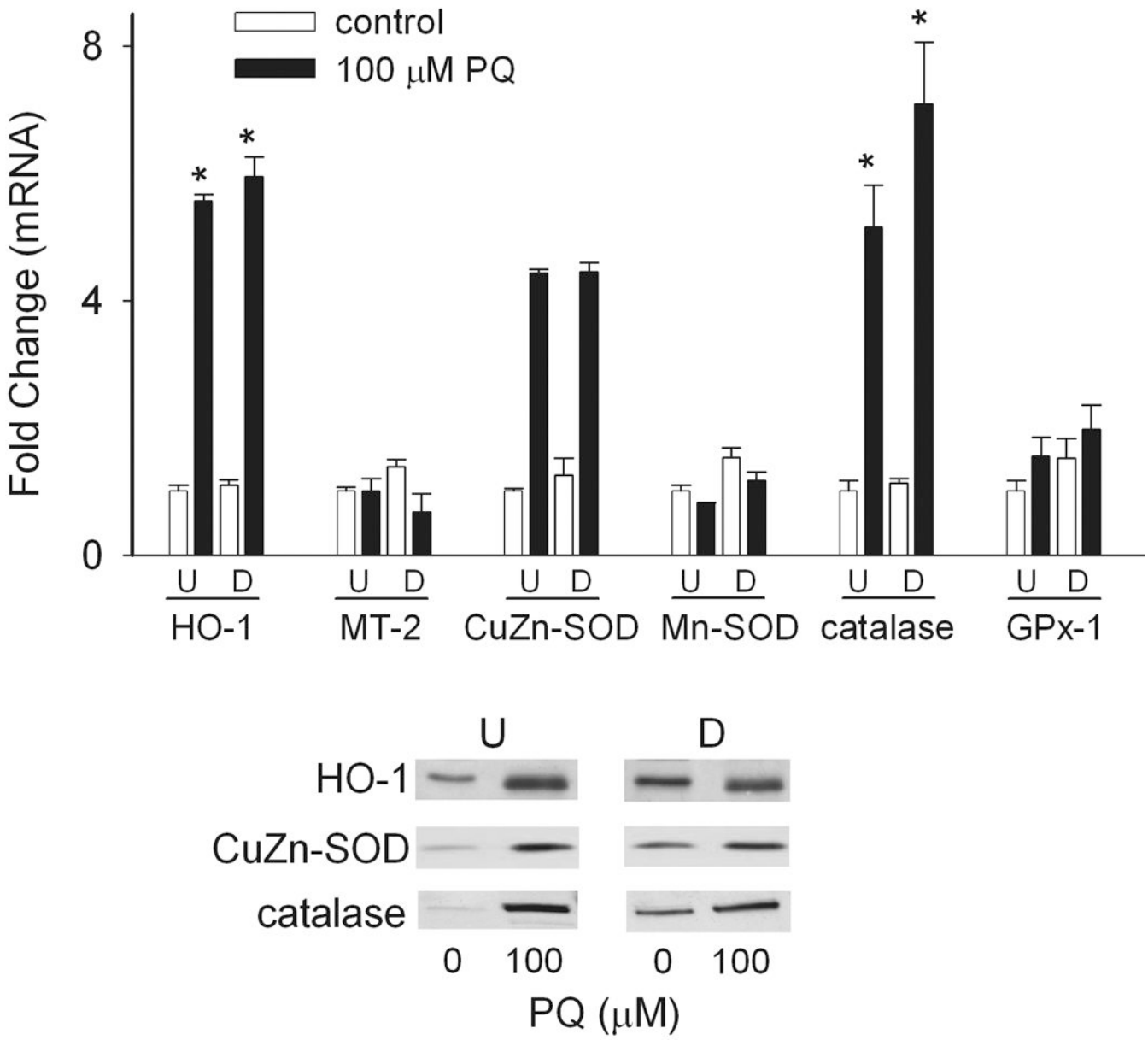

Figure 8. Effects of paraquat on expression of antioxidant enzymes

Undifferentiated (U) and differentiated (D) keratinocytes were treated with 100 μM paraquat or control. After 24 h, mRNA was extracted and analyzed for gene expression by real-time PCR (upper panel) or total cellular lysates were prepared and protein expression was analyzed by Western blotting (lower panel). Loading of equal amounts of protein was confirmed by silver staining of the gels. *$p < 0.05$, undifferentiated control cells versus paraquat-treated undifferentiated and differentiated cells. Each bar represents the mean ± SE (n = 3).

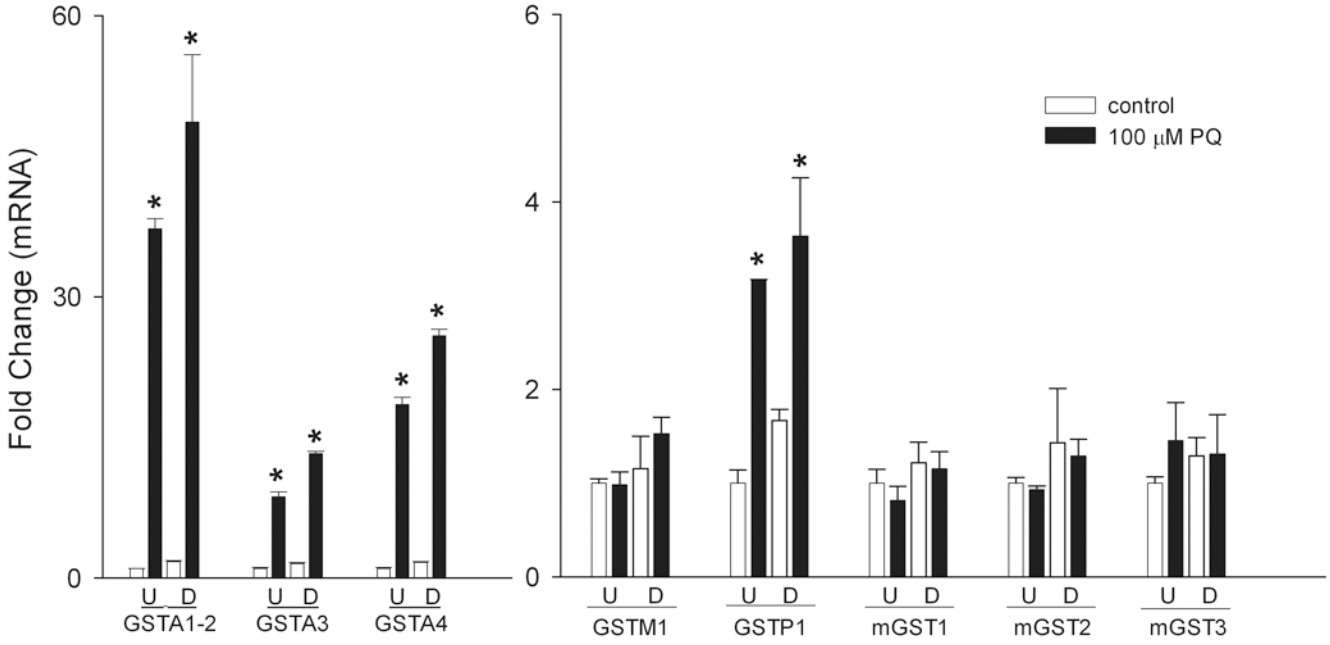

Figure 9. Effects of paraquat on keratinocyte expression of glutathione-S-transferases

Undifferentiated (U) and differentiated (D) keratinocytes were treated with 100 μM paraquat or control. After 24 h, mRNA was extracted and analyzed for gene expression by real-time PCR. *Left panel*: Effects of paraquat on mRNA expression of GSTA1-2, GSTA3 and GSTA4. *Right panel*: Effects of paraquat on mRNA expression of GSTM1, GSTP1, mGST1, mGST2 and mGST3. *$p < 0.05$, undifferentiated control cells versus paraquat-treated undifferentiated and differentiated cells; § $p < 0.05$, undifferentiated paraquat-treated cells versus differentiated paraquat-treated differentiated cells. Each bar represents the mean ± SE (n = 3).